© 2016. Published by The Company of Biologists Ltd | Journal of Cell Science (2016) 129, 2239-2249 doi:10.1242/jcs.182477

RESEARCH ARTICLE

The central element of the synaptonemal complex in mice is organized as a bilayered junction structure

Abrahan Hernández-Hernández[1], Sergej Masich[1], Tomoyuki Fukuda[1,2], Anna Kouznetsova[1], Sara Sandin[3], Bertil Daneholt[1] and Christer Höög[1,*]

ABSTRACT

The synaptonemal complex transiently stabilizes pairing interactions between homologous chromosomes during meiosis. Assembly of the synaptonemal complex is mediated through integration of opposing transverse filaments into a central element, a process that is poorly understood. We have, here, analyzed the localization of the transverse filament protein SYCP1 and the central element proteins SYCE1, SYCE2 and SYCE3 within the central region of the synaptonemal complex in mouse spermatocytes using immunoelectron microscopy. Distribution of immuno-gold particles in a lateral view of the synaptonemal complex, supported by protein interaction data, suggest that the N-terminal region of SYCP1 and SYCE3 form a joint bilayered central structure, and that SYCE1 and SYCE2 localize in between the two layers. We find that disruption of SYCE2 and TEX12 (a fourth central element protein) localization to the central element abolishes central alignment of the N-terminal region of SYCP1. Thus, our results show that all four central element proteins, in an interdependent manner, contribute to stabilization of opposing N-terminal regions of SYCP1, forming a bilayered transverse-filament–central-element junction structure that promotes synaptonemal complex formation and synapsis.

KEY WORDS: Meiosis, Synaptonemal complex, Homologous chromosomes, Immunoelectron microscopy

INTRODUCTION

The meiotic cell division process in germ cells gives rise to haploid, genetically diverse gametes (Handel and Schimenti, 2010). The haploid state is accomplished through two sequential cell divisions, meiosis I and II, which occur without an intervening DNA replication step. The homologous chromosomes (homologues) become separated at the first meiotic division (meiosis I), whereas the sister chromatids separate from each other at the second meiotic division (meiosis II). Missegregation of chromosomes gives rise to aneuploid germ cells, a common cause of infertility and developmental disabilities (Handel and Schimenti, 2010; Nagaoka et al., 2012). The accuracy of the chromosome segregation process is enforced by a crossover recombination mechanism that promotes chromosome alignment and introduces physical DNA linkages (chiasmata) between the homologues (Zickler and Kleckner, 2015).

[1]Department of Cell and Molecular Biology, Karolinska Institutet Berzelius väg 35, Stockholm 171 77, Sweden. [2]Graduate School of Biological Sciences, Nara Institute of Science and Technology, Ikoma, Nara 630-0192, Japan. [3]School of Biological Sciences, Nanyang Technological University, 60 Nanyang Drive, 637551, Singapore.

*Author for correspondence (Christer.hoog@ki.se)

C.H., 0000-0003-0872-1374

Received 23 October 2015; Accepted 14 April 2016

During the prophase stage of meiosis I (prophase I), an elaborate proteinaceous structure assembles onto the chromosomes. This meiosis-specific structure, called the synaptonemal complex, is conserved from yeast to mammals (Westergaard and von Wettstein, 1972; Zickler and Kleckner, 1999). The synaptonemal complex stabilizes the pairing interactions between the homologues (in a process called synapsis) and promotes crossover recombination and chiasmata formation (Zickler and Kleckner, 2015). Examinations of meiocytes at the pachytene stage of prophase I using transmission electron microscopy have shown that the synaptonemal complex has a tripartite organization that extends along the entire length of the synapsed homologues. The tripartite synaptonemal complex structure comprises a central element flanked by two parallel lateral elements. The region in between the lateral elements is referred to as the central region, where the two opposing lateral elements are separated by approximately 100 nm (Moses, 1956; Westergaard and von Wettstein, 1972). The lateral element (also called an axial element prior to synapsis) is part of a cohesin-based chromosome axis that holds the sister chromatids of the homologues together (McNicoll et al., 2013). The axes of the chromosomes are interconnected along their entire length by transverse filaments – fine filamentous structures that span the width of the central region of the synaptonemal complex – generating a zipper- or ladder-like structure (Hawley, 2011).

Studies in several model organisms have identified proteins that constitute the transverse filaments and that are essential for synaptonemal complex formation and synapsis, including SYCP1 in mammals (Meuwissen et al., 1992), ZIP1 in *Saccharomyces cerevisiae* (Sym et al., 1993), C(3)G in *Drosophila melanogaster* (Page and Hawley, 2001), ZYP1 in *Arabidopsis thaliana* (Osman et al., 2006) and SYP-1, SYP-2, SYP-3 and SYP-4 in *Caenorhabditis elegans* (Colaiacovo et al., 2003; MacQueen et al., 2002; Schild-Prufert et al., 2011; Smolikov et al., 2007, 2009). The transverse filament proteins in the different organisms share a similar predicted secondary structure, having an extended central α-helical domain (predicted to form coiled-coil structures) with flanking N- and C-terminal regions. Immunoelectron microscopy analysis, using domain-specific antibodies, of the organization of the transverse filament proteins within the central region of the synaptonemal complex in *S. cerevisiae*, *D. melanogaster* and mouse have shown that the transverse filament proteins (which are most likely to be present as homodimers) are organized in a head-to-head arrangement – the N-terminal domains positioned within the central element and the C-terminal domains localized within the two opposing chromosome axes (Anderson et al., 2005; Dong and Roeder, 2000; Liu et al., 1996; Schmekel et al., 1996). The role of the N-terminal region of the transverse filament proteins in synapsis of homologous chromosomes seems to differ between organisms. Deletion of the N-terminal region of C(3)G in *D. melanogaster* prevents synaptonemal complex

Journal of Cell Science

Journal of Cell Science (2016) 129, 2239-2249 doi:10.1242/jcs.182477

formation (Jeffress et al., 2007), whereas deletion of the N-terminal region of ZIP1 in *S. cerevisiae* has minor effects on synaptonemal complex formation (Tung and Roeder, 1998).

A fibrous network has been described within the central element of the synaptonemal complex in insects that seemingly connect layers of transverse filaments stacked on top of each other in longitudinal, lateral and transverse directions (Schmekel and Daneholt, 1995; Schmekel et al., 1993a,b; Solari and Moses, 1973). Several proteins that might contribute to the formation of this fibrous network have been identified, including SYCE1, SYCE2, SYCE3 and TEX12 in mice (Costa et al., 2005; Hamer et al., 2006; Schramm et al., 2011), Ecm11 and Gmc2 in *S. cerevisiae* (Humphryes et al., 2013), and CONA and Corolla in *D. melanogaster* (Collins et al., 2014; Page et al., 2008). These proteins have been shown by immunoelectron microscopy studies to localize to the central element of the synaptonemal complex and by genetic studies to be required for synaptonemal complex assembly. These results strongly suggest that these proteins, tentatively assigned as central element proteins, act to stabilize interactions between opposing transverse filaments within the central element of the synaptonemal complex (Bolcun-Filas et al., 2007, 2009; Collins et al., 2014; de Vries et al., 2005; Hamer et al., 2008; Humphryes et al., 2013; Page et al., 2008; Schramm et al., 2011). In *C. elegans*, the four different transverse filament proteins have been shown to interact in a staggered and interdependent manner, generating a central region structure that connects the opposing lateral elements of the synaptonemal complex (Schild-Prufert et al., 2011).

The localization patterns for SYCP1 and the central element proteins have been analyzed in *Sycp1*-, *Syce1*-, *Syce2*-, *Syce3*- and *Tex12*-null mouse meiocytes (Costa et al., 2005; Bolcun-Filas et al., 2007, 2009; Hamer et al., 2008; Schramm et al., 2011). The results of these experiments suggest that synaptonemal complex assembly in mice takes place in a sequential order – i.e. SYCP1 recruits SYCE3, followed by recruitment of SYCE1, and lastly by recruitment of SYCE2–TEX12 to generate a transverse-filaments–central-element protein complex (Costa and Cooke, 2007; Fraune et al., 2012). Direct protein–protein interactions that have been established between transverse filaments and central element proteins have been studied using *in vitro* and *in vivo* protein-binding experiments, as well as by using biophysical assays. Two groups of strongly interacting proteins within the central element of the synaptonemal complex, SYCE3–SYCE1 and SYCE2–TEX12, have been identified using several independent assays (Davies et al., 2012; Hamer et al., 2006; Lu et al., 2014; Schramm et al., 2011). Interactions between the N-terminus of SYCP1 and SYCE1, as well as between the N-terminus of SYCP1 and SYCE2, have been identified *in vitro* (Costa et al., 2005). However, yeast two-hybrid studies have failed to identify interactions between SYCP1 and SYCE1 or SYCE2 (Davies et al., 2012), raising the question whether or not SYCP1 directly interacts with SYCE1 or SYCE2.

Here, we have analyzed the three-dimensional (3D) localization of transverse filaments and central element proteins within the central region of the synaptonemal complex in wild-type mouse spermatocytes using immunoelectron microscopy. We found that the N-terminal regions of SYCP1 and SYCE3 display an overlapping bimodal pattern of distribution, when the synaptonemal complex is analyzed in a lateral view. The N-terminal region of SYCP1 (SYCP1-N) interacts with SYCE3 *in vitro* and when coexpressed in mammalian cell culture cells, suggesting that the two proteins jointly establish a bilayered junction structure within the central element of the synaptonemal complex. In contrast, we found SYCE1 and SYCE2 to both display a monomodal distribution pattern in a lateral view of the synaptonemal complex, and to be localized in between the bilayered structures formed by the N-terminal regions of SYCP1 and SYCE3. We find that the presence of SYCE2 and TEX12 is crucial for central alignment of the N-terminal region of SYCP1 and SYCE1 in between closely aligned homologous chromosomes. Our results therefore show that the N-terminal region of SYCP1 and the central element proteins establish a multilayered structure, where all four central element proteins, in an interdependent manner, are required for transverse stabilization of the N-terminal regions of SYCP1 and for synapsis.

RESULTS

The central element of the synaptonemal complex in insects (in a longitudinal or a lateral geometrical view along the synaptonemal complex) has been shown by electron microscopy and 3D electron microscopy analyses to be organized in several identical layers stacked on top of each other (Rasmussen, 1976; Schmekel and Daneholt, 1995; Schmekel et al., 1993a,b). We have here, by using immunoelectron microscopy, analyzed the 3D organization of the mouse central element proteins SYCE1, SYCE2 and SYCE3 in the synaptonemal complex. The axes of synapsed homologous chromosomes coil or twist, forming helix-like structures (Schucker et al., 2015; Westergaard and von Wettstein, 1972), revealing alternating frontal and lateral views of the synaptonemal complex in serial sections of mouse spermatocytes (Fig. 1; Fig. S1).

The immunoelectron microscopy experiments were performed on ultrathin sections of plastic-embedded testicular tissue, a method that provides more reliable results than the use of surface-spread spermatocytes (Schmekel et al., 1996). Mouse testis sections containing seminiferous tubules between stages IV and VIII of the seminiferous epithelial cycle, stages at which primary spermatocytes have reached the pachytene stage, were incubated with primary antibodies against SYCE1, SYCE2 and SYCE3, and with secondary antibodies coupled to 5-nm gold particles (TEX12 was not analyzed here because the number of observed gold particles was insufficient for a more detailed analysis of its localization within the central element). The epitope regions within SYCE1, SYCE2 and SYCE3 that are recognized by the primary antibodies have been summarized in Fig. S2. The ultrathin sections provide a smooth surface, and neither antibodies nor gold particles can penetrate into the plastics (Newman and Hobot, 2001). The antibody–antibody–gold complex is flexible and can attain any conformation, and gold particles bound to the plastic surface will therefore be isotropically distributed within a circular area with a radius of 20–25 nm, with the antigen in the center (Harris et al., 1998; Krijnse Locker and Schmid, 2013; Roux, 1999; Wolf et al., 2012).

We first analyzed the localization of SYCE1, SYCE2 and SYCE3 within the central element in a lateral view of the synaptonemal complex (Fig. 1; Fig. S1). For the analysis of the synaptonemal complex from a lateral view, we selected regions where a distinct central element was observed, flanked in both directions by tri-partite synaptonemal complex structures (either in the same section or in the serial sections above and below). We did not include transition regions close to the flanking tri-partite structures in our analysis (Fig. S1). Lateral views of the central element of the synaptonemal complex were only included when the observed central element structure had a variation in height between 30 and 47 nm (average height was 38 nm). To determine the exact distribution of gold particles in lateral views of the central element, the distance between each gold particle to the closest

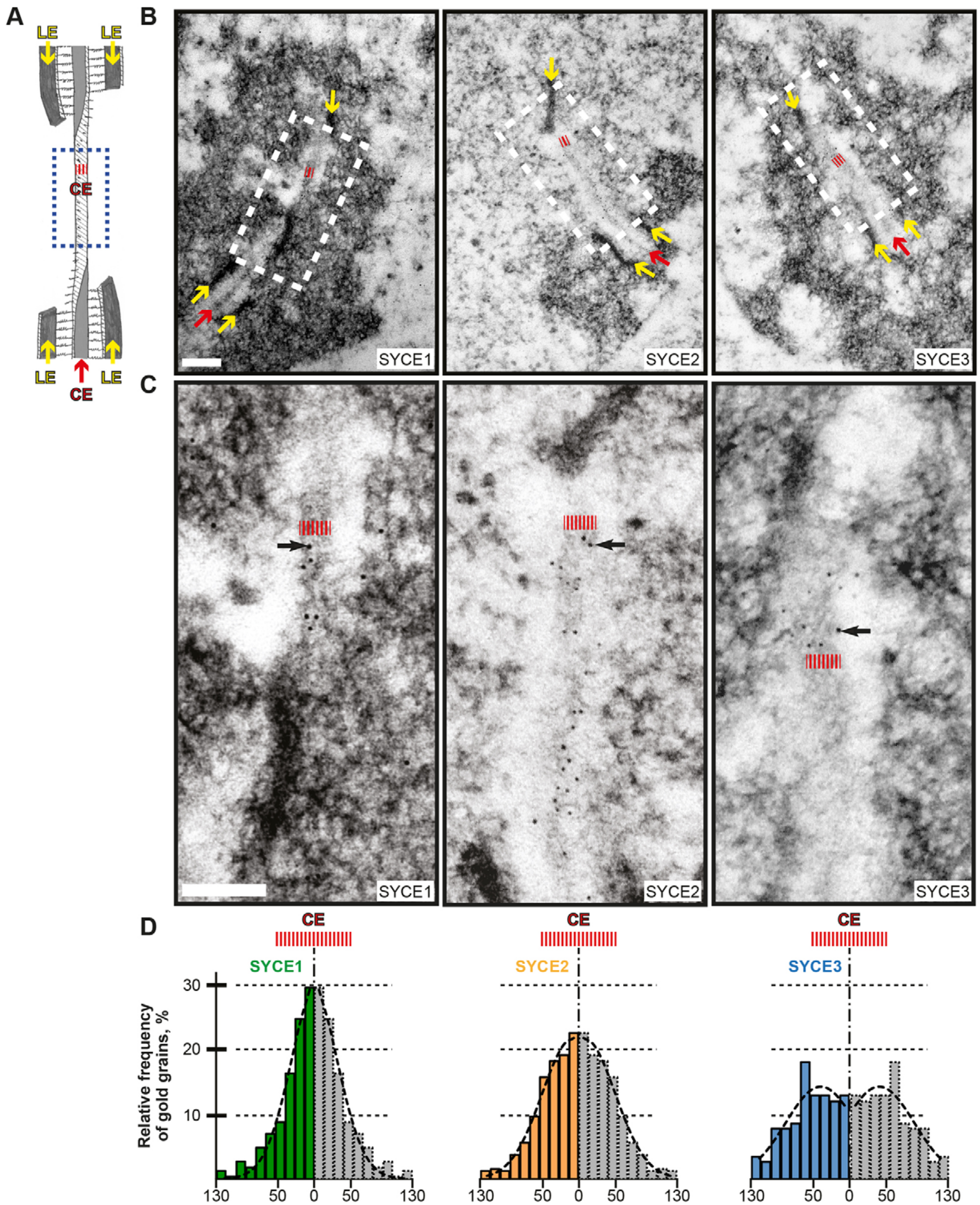

Fig. 1. Immunoelectron microscopy localization of the central element proteins in a lateral view of the central element. (A) Schematic drawing of a twisted segment of a central element (CE) examined following ultrathin sectioning of a synaptonemal complex. A central lateral view of the central element (blue dashed box) is flanked by frontal views displaying a classic tripartite organization [two lateral elements (LE) separated by a central element]. The height of the central element in a lateral view is outlined by a dashed red line. (B) Immunoelectron microscopy analysis of three central elements (dashed white boxes) in lateral views of synaptonemal complexes, with the height of the central elements (red dashed lines) indicated, using antibodies against SYCE1, SYCE2 and SYCE3. Adjacent frontal views displaying a tripartite organization are indicated with red (central elements) and yellow (lateral elements) arrows. Scale bar: 100 nm. (C) Higher magnification images of the lateral view of the central elements within the dashed white boxes shown in B. The gold particles represent the position of the three antibodies used (against SYCE1, SYCE2 and SYCE3, respectively). For each antibody, one representative gold particle has been indicated with a black arrow. A dashed red line denotes the central element. Scale bar: 100 nm. (D) Histograms showing the distribution of gold particles within the central element (red dashed line) using antibodies against SYCE1 (green columns), SYCE2 (orange columns) or SYCE3 (blue columns). The recorded distributions are mirrored (in gray) to relate the data to the symmetric synaptonemal complex structure. The fitting curves for each distribution are shown in black. The position of the central element along the horizontal axis is indicated with a dashed red line above the histogram. The number of gold particles measured was 221 for SYCE1, 390 for SYCE2 and 115 for SYCE3. Synaptonemal complexes were from different samples and from at least two different wild-type mice.

Journal of Cell Science (2016) 129, 2239-2249 doi:10.1242/jcs.182477

central element border was measured and compared to the overall distance between the edges of the central element. Because the distance between the central element borders (central element height in a lateral view) varies for each synaptonemal complex sample, the central element height was normalized to 100 units, and the distance from the gold particle to the closest central element border was recalculated. Owing to the lateral resolution imposed by the antibody–antibody complex, deposition of gold particles outside the central element are expected and, to account for these, a region of 80 units (31 nm) outside of the central element borders was included in our analysis. The normalization of distances allows for standardization of the measurements, which is necessary given the slight variations in width between lateral elements in different sample preparations (Schild-Prufert et al., 2011; Schmekel et al., 1996). The normalization results in values between 0 and 130, with 0 corresponding to the center of the central element height, 50 to the border of the central element and 130 to the total span of the analyzed region. The normalized distance was divided into intervals of 13 units, each corresponding to 5 nm. The number of particles in each interval was expressed as a percentage of all particles recorded (relative particle frequency). The results are presented as histograms showing the relative particle frequency in the ten intervals covering the distance from the center to the border of the central element (0 to 50) plus the additional analyzed region outside the central element border (50 to 130). The obtained distribution of gold particles was mirrored relative to the center of the central element.

We found that the gold particles representing SYCE3 accumulated in a bimodal pattern, where the two peaks of the gold distribution pattern localized towards the outside borders of the central element (in a lateral view representing the top and bottom parts of the central element) (Fig. 1). In contrast, the gold particles representing SYCE1 and SYCE2 displayed a monomodal pattern localized at a central position within the central element (Fig. 1). Thus, analysis of the distribution patterns of the gold particles representing the three different central element proteins in a lateral view of the synaptonemal complex indicates a layered organization, where SYCE3 defines the top and bottom parts of the central element, and SYCE2 and SYCE3 localize in between the two layers defined by SYCE3.

The localization of the gold particles that correspond to SYCE1, SYCE2 and SYCE3 was also determined in a frontal view of the synaptonemal complex (Fig. S3). The distribution of gold particles within the central region of the synaptonemal complex was determined based on the localization of individual gold particles relative to the center of the nearest axial structure, followed by normalization of the distance between the opposing axial structures at the position of each individual gold particle (Schmekel et al., 1996). We used in this analysis only gold particles that were present in regions of the synaptonemal complex where a central element was surrounded by two opposing lateral elements, representing a classic frontal view perspective of the synaptonemal complex, to avoid synaptonemal complex regions that were highly tilted as a result of the helical organization of this structure. Because the distance between the centers of the lateral element varies for each synaptonemal complex sample, with an average distance of 168.5 nm (ranging in between 142 nm and 194 nm), the distance between the opposing lateral elements was normalized to 100 units (where on average 1 unit then corresponds to 1.7 nm), and the distance for each gold particle to the center of the nearest lateral element was then recalculated. Our results are in close agreement with similar analysis made in rat where the average distance between the centers of opposing lateral elements was found to be 180 nm and where 1 unit was found to correspond to 1.8 nm (Schmekel et al., 1996). The normalization results in values between 0 and 50, with 0 corresponding to the center of the lateral element and 50 to the middle of the central region of the synaptonemal complex in between the opposing lateral elements. The normalized distance was divided into intervals of 3 units, corresponding to 5 nm, except for the first interval (representing background level) that comprised 2 units (3.4 nm). To compare the distributions of gold particles that represented different antibodies, the number of particles in each interval was expressed as a percentage of all particles recorded (relative particle frequency). The results are presented as histograms showing the relative particle frequency in the 17 classes covering the distance from one lateral element center to the center of the central region (0–50 units on the horizontal axis). To relate the gold distribution to the symmetric synaptonemal complex structure, the recorded distribution of gold particles is mirrored (in gray) relative to the center of the central region in the histogram (at the position of 50 units). The width of the central element was measured for every analyzed synaptonemal complex, and the average width amounted to 26 nm, indicated under the horizontal axes of the histograms (Fig. S3).

Our analysis of the distribution of the gold particles representing the three central element proteins in a frontal view of the synaptonemal complex strongly suggests that SYCE1, SYCE2 and SYCE3 are localized within the central element of the synaptonemal complex (Fig. S3), results that are in agreement with earlier studies (Costa et al., 2005; Schramm et al., 2011). We were unable to identify a bimodal distribution for any of the central element proteins in a frontal view.

The N-terminal region of SYCP1 displays a bimodal distribution pattern in a lateral view of the synaptonemal complex

We next set out to determine the relative localization of the N-terminal region of the transverse filament protein SYCP1 with immunoelectron microscopy, in frontal and lateral views of the synaptonemal complex. The mouse SYCP1 protein has a length of 993 amino acids, with a predicted coiled-coil region that spans amino acid residues 116–815 (Fraune et al., 2012; Meuwissen et al., 1992). Pachytene spermatocytes were incubated with primary antibodies that recognized amino acid at positions 53–128 within the N-terminal region of SYCP1 and secondary antibodies coupled to 5-nm gold particles. We first analyzed the distribution of the gold particles representing the N-terminal region of SYCP1 in a lateral view of the synaptonemal complex, following the same approach as discussed above for the localization of the central element proteins in a lateral view. We observed here a bimodal pattern for the N-terminal region of SYCP1 overlapping with the one found for SYCE3 in the central element (Fig. 2). Our results therefore suggest that SYCE3 and the N-terminal region of SYCP1 are part of a bilayered transverse structure that connects opposing transverse filaments with the central element.

We next analyzed the distribution of the gold particles representing the N-terminal region of SYCP1 in a frontal view of the synaptonemal complex, following the same methodological approach as described for the analysis of the distribution of central element proteins in a frontal view (see above). We found the gold particles representing the N-terminal region of SYCP1 to be localized to the central element of the synaptonemal complex (Fig. S4), results that are in agreement with previous studies (Liu

Journal of Cell Science

Journal of Cell Science (2016) 129, 2239-2249 doi:10.1242/jcs.182477

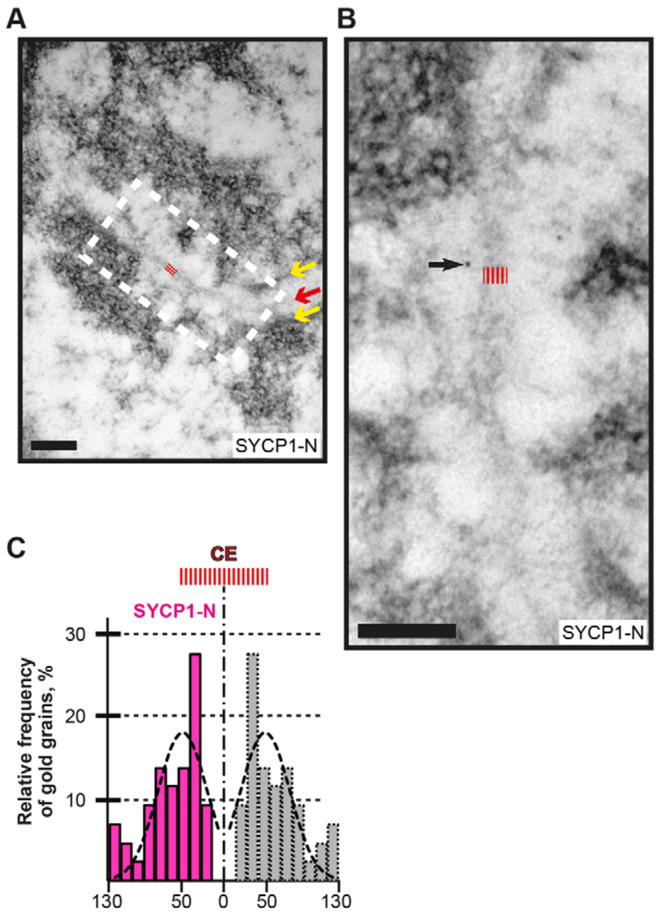

Fig. 2. Immunoelectron microscopy localization of the N-terminal region of SYCP1 in a lateral view of the central element. (A) Immunoelectron microscopy analysis of the central element (dashed red line) in a lateral view of a synaptonemal complex (dashed white box) using an antibody against the N-terminus of SYCP1 (SYCP1-N). An adjacent frontal view that shows a tripartite organization is indicated with red (central element, CE) and yellow (lateral elements) arrows. Scale bar: 100 nm. (B) Higher magnification image of the lateral view of the central element within the dashed white box in A. One representative gold particle has been indicated with a black arrow. A dashed red line outlines the central element. Scale bar: 100 nm. (C) Histogram showing the distribution of gold particles within the central element (red dashed line) seen in a lateral view of the synaptonemal complex using an antibody against the N-terminal region of SYCP1 (pink columns). The recorded distribution is mirrored (in gray) to relate the data to the symmetrical synaptonemal complex structure. There is a single striking divergence in the distribution of the gold particles close to the center of the central element that we cannot explain. The fitting curve is shown in black. 43 gold particles were included in the analysis, which were from synaptonemal complexes of different samples and from two wild-type mice.

et al., 1996; Schmekel et al., 1996). It was not possible in this analysis to determine whether or not the N-terminal region of SYCP1 displays overlapping or separating distribution patterns within the central element.

SYCE3 interacts with the N-terminal region of SYCP1

The bimodal distribution patterns shown for SYCE3 and the N-terminal region of SYCP1 in a lateral view of the synaptonemal complex indicate that the two proteins interact with each other. Knockout experiments and protein localization data have previously suggested that SYCE3 acts as an intermediary protein connecting the N-terminus of SYCP1 with SYCE1 (Schramm et al., 2011); however, no direct *in vitro* interactions between the N-terminus of SYCP1 (amino acids 1–200) and SYCE3 have been previously identified (Schramm et al., 2011). We have here analyzed whether the two proteins directly interact using *in vitro* protein–protein interaction studies and protein coexpression assays. The N-terminal amino acids 1–400 of SYCP1 were fused to a FLAG peptide and tested for protein–protein interactions against SYCE1, SYCE2, SYCE3 and TEX12 (each protein fused to the GST protein), using an *in vitro* GST pulldown assay (Fig. 3A). We found that the N-terminal region of SYCP1 interacted with SYCE3, but not with SYCE1, SYCE2 or TEX12. Thus, our experiments identified an *in vitro* interaction between the N-terminal region of SYCP1 (1–400) and SYCE3, indicating that a region within the N-terminal 121–400 amino acids of SYCP1, which includes the first and second predicted coiled-coil domains (Fraune et al., 2012), preferentially contributes to this interaction.

SYCP1 has previously been shown to give rise to cytoplasmic aggregates and to filamentous structures when ectopically expressed in mammalian cell culture cells (Ollinger et al., 2005; Yuan et al., 1996). We took advantage of this observation and analyzed whether interactions between SYCP1 and the four different central element proteins could be identified following their co-transfection into COS-7 cells (Fig. 3B–H). The expression patterns for the five different proteins were monitored using immunofluorescence microscopy following transfection of COS-7 cells (Fig. 3B,C). Expression of SYCP1 gave rise to filamentous structures in transfected cells (Fig. 3B), this is in contrast to the individual central element proteins, which formed foci or gave rise to diffuse nuclear or cytoplasmic staining patterns in the transfected cells (Fig. 3C). We next co-transfected SYCP1 with each of the four different central element proteins separately (Fig. 3D–G) in order to find out if any of the central element proteins would become colocalized with the filamentous structures formed by SYCP1. Strikingly, SYCE3 localized to the filamentous structures formed by SYCP1 following their coexpression in COS-7 cells (Fig. 3F), whereas such a colocalization pattern could not be observed for SYCE1, SYCE2 and TEX12 following their coexpression with SYCP1 (Fig. 3D,E,G). Our results suggest that SYCE3, not SYCE1 or SYCE2, directly interacts with SYCP1; results that are in agreement with results of mouse knockout experiments that show that SYCE3 is essential for recruitment of SYCE1 and SYCE2 to the synaptonemal complex (Schramm et al., 2011). Previous analysis using *in vitro* protein interaction experiments has identified interactions between the first 200 amino acids of SYCP1 (including the first coiled-coil domain) and SYCE1, as well as between SYCP1 and SYCE2, *in vitro* (Costa et al., 2005). However, in agreement with our results, interactions between SYCP1 and SYCE1 or between SYCP1 and SYCE2 have not been observed when analyzed using yeast two-hybrid methods (Davies et al., 2012).

SYCE3 and SYCE1 have been shown to interact *in vitro* using several different assays (Lu et al., 2014; Schramm et al., 2011). We tested whether SYCE3 could bring SYCP1 together with SYCE1 in COS-7 cells that coexpressed all three proteins simultaneously (Fig. 3H). The localization patterns for the three proteins were analyzed using immunofluorescence microscopy, and we found that coexpression of SYCE3 with SYCE1 resulted in the localization of both proteins to filamentous structures formed by SYCP1 in COS-7 cells (Fig. 3H). Thus, SYCE3 promotes assembly of a joint protein complex comprising SYCP1, SYCE3 and SYCE1 when the three proteins are coexpressed in mammalian cell culture cells.

Journal of Cell Science (2016) 129, 2239-2249 doi:10.1242/jcs.182477

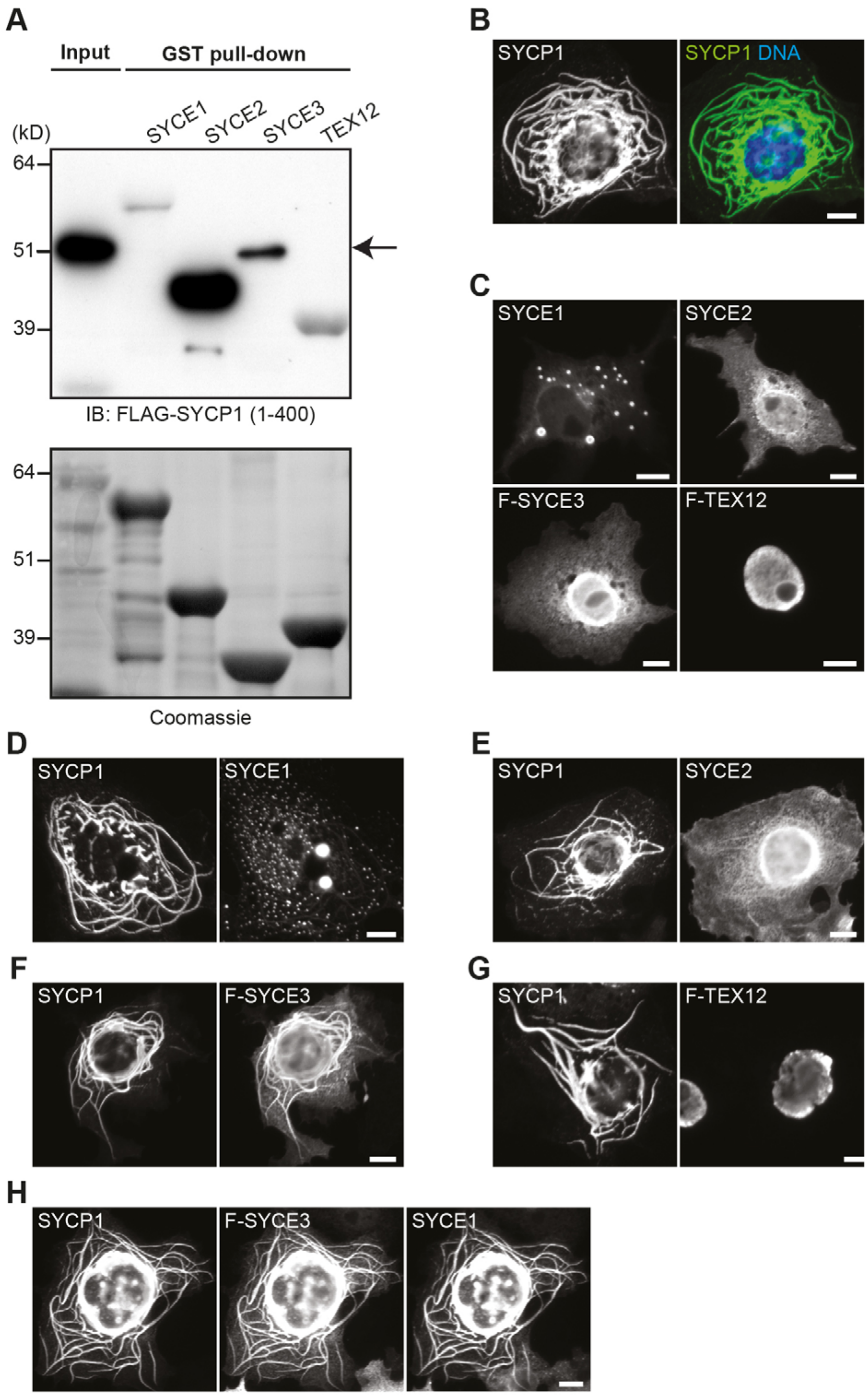

Fig. 3. SYCP1 and SYCE3 interact *in vitro* and *ex vivo*. (A) *In vitro* GST pulldown assay. SYCE1, SYCE2, SYCE3 and TEX12 were fused to the GST protein and used as bait to test interactions with the N-terminal region of SYCP1 (amino acids residues 1–400) fused to FLAG peptide. Protein complexes were separated using SDS-PAGE, and western blotting (IB) was performed using anti-FLAG antibody. The assay identifies an interaction between SYCE3 and the N-terminal region of SYCP1 (upper panel in A). The position of the SYCP1(1–400)–FLAG fusion protein on the western blot is indicated by an arrow. The additional bands on the western blot labeled with the anti-FLAG antibody (in the lanes labeled SYCE1, SYCE2 and TEX12) are most likely to represent weak interactions between the antibody and the excessive amount of GST-fusion proteins (or degradation thereof). Coomassie staining was performed to visualize expressed GST-fusion proteins (lower panel in A). (B–H) *Ex vivo* expression and coexpression of the central element proteins SYCE1, SYCE2, SYCE3, TEX12 and the transverse filament protein SYCP1 in the cytoplasm of COS-7 cells. Immunolabeling was performed using antibodies against SYCP1, SYCE1, SYCE2 and FLAG (for FLAG-tagged SYCE3 and TEX12). SYCP1 was the only protein that formed a filamentous structure in the cytoplasm of COS-7 cells when expressed alone (B and C). SYCE3, but not SYCE1, SYCE2 or TEX12, colocalized with the filamentous structures formed by SYCP1 when the proteins coexpressed (D–G). SYCP1–SYCE3 filamentous structures recruit SYCE1 (H). Protein expression was monitored by immunofluorescence microscopy following transfection of COS-7 cells. Scale bars: 10 µm.

SYCE2 and TEX12 are essential for spatial confinement of the N-terminal region of SYCP1 in between aligned homologous chromosomes

Previous work has shown that in the absence of SYCE1 or SYCE3 in mutant mice, SYCP1 displays a discontinuous pattern along unsynapsed chromosomes (Bolcun-Filas et al., 2009; Schramm et al., 2011). This is in contrast to the situation in the absence of SYCE2 or TEX12, when SYCP1, SYCE1 and SYCE3 localize to short central-element-like structures present in between aligned homologous chromosomes (Bolcun-Filas et al., 2007; Hamer et al., 2008; Schramm et al., 2011). These results have been interpreted to suggest that SYCP1, SYCE1 and SYCE3 together establish synapsis initiation sites and promote limited longitudinal polymerization of transverse filaments, whereas SYCE2 and TEX12 would be required for extended synaptonemal complex formation (Costa and Cooke, 2007; Fraune et al., 2012).

We have here by immunoelectron microscopy, in more detail, analyzed the organization of the central region between closely aligned lateral elements in *Tex12*-null spermatocytes – i.e. in a situation when TEX12 and its binding partner SYCE2 become

Journal of Cell Science (2016) 129, 2239-2249 doi:10.1242/jcs.182477

displaced from meiotic chromosomes (Hamer et al., 2008). *Tex12*-null pachytene spermatocytes were incubated with antibodies against the N-terminal region of SYCP1 and SYCE1, and with secondary antibodies fused to 5-nm gold particles. The distributions of the gold particles were then determined relative to the axes of the chromosomes represented by the lateral elements (Fig. 4). The lateral elements analyzed in the mutant spermatocytes were aligned at a distance similar to the one seen in wild-type spermatocytes, where the distance in between the centers of the opposing lateral elements where on average 162 nm in *Tex12*-null spermatocytes and 168.5 nm on average in wild-type spermatocytes. To determine the exact distribution of gold particles in between closely aligned lateral elements in a frontal view of the synaptonemal complex in *Tex-12*-null spermatocytes, we followed a similar approach as used when the localization of the N-terminal region of SYCP1 and SYCE1 in wild-type spermatocytes was determined (see above, Figs S3 and S4). The distance between each gold particle and the closest lateral element center was measured and compared to the overall distance between the centers of the two lateral elements at the same position. Because the distance between the centers of the two lateral elements varies between 142 and 196 nm (with an average distance of 162 nm) in samples, the distance between the centers of the lateral elements was normalized to 100 units (on average, 1 unit corresponds to 1.6 nm), and the distance from the gold particle to the center of the closest lateral element was recalculated. The normalization resulted in values between 0 and 50, with 0 corresponding to the center of the lateral element and 50 to the middle of the central region in between the aligned lateral elements. The normalized distance was divided into intervals of 3.1 units corresponding to 5 nm, except for the first class, which comprised 0.4 units (0.6 nm). In order to compare the distribution of gold particles for the antibodies representing the two different proteins, the number of particles in each interval was expressed as the percentage of all particles recorded (relative particle frequency). The results are presented as histograms showing the relative particle frequency in the 17 intervals covering the distance from one lateral element center to the center of the central-element-like structure (0–50 units on the horizontal axis). To relate the distribution of gold particles to the symmetric synaptonemal complex structure, the recorded distribution of gold particles was mirrored (in gray) relative

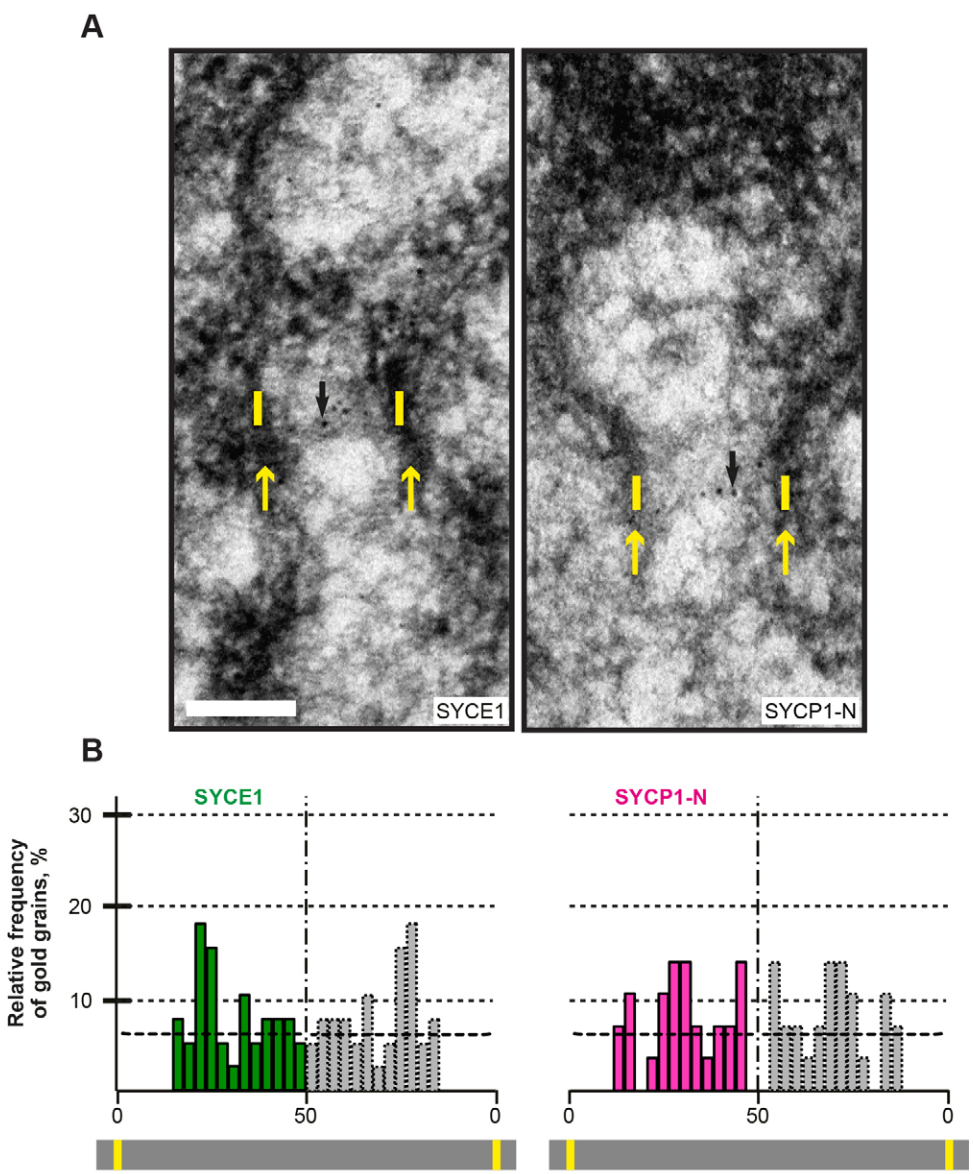

Fig. 4. Immunoelectron microscopy analysis of the location of the N-terminal region of SYCP1 and SYCE1 in a frontal view of the synaptonemal complex in *Tex12*-null pachytene spermatocytes. (A) Immunoelectron microscopy analysis using antibodies against the N-terminal region of SYCP1 (SYCP1-N) and SYCE1 in frontal views of aligned lateral elements in *Tex12*-null pachytene spermatocytes. Black arrows in each panel indicate a representative gold particle. Yellow arrows indicate lateral elements, and the yellow vertical lines demarcate the center of each one of the opposing lateral elements. Scale bar: 100 nm. (B) Histograms showing the distribution of gold particles in between the opposing lateral elements in frontal sections using antibodies against SYCE1 (green columns) and the N-terminal region of SYCP1 (SYCP1-N, magenta columns). A mirrored distribution (in gray) has been added to relate the data to the symmetric synaptonemal complex structure. The random distribution fitting lines for each distribution are indicated with dashed black horizontal lines. The yellow vertical lines within the gray box below the histogram represent the centers of the lateral elements and thus the position of the two zeros on the horizontal axes. The histograms were based on the following number of particles recorded: 38 for SYCE1 and 28 for SYCP1-N, taken from different samples and from several different *Tex12*-null mice.

to the center of the central-element-like structure in the histogram (at position 50 units).

We found the gold particles that represent SYCE1 and the N-terminus of SYCP1 uniformly labeled the central region in between aligned lateral elements in *Tex12*-null spermatocytes (Fig. 4). Importantly, there was no evidence for a restricted localization of SYCE1 or the N-terminal region of SYCP1 to a central position in between the aligned lateral elements, as seen in wild-type spermatocytes (compare Fig. 4B versus Figs S3C and S4D). Furthermore, statistical comparison of gold-grain distributions corresponding to SYCE1 and SYCP1-N in wild-type versus *Tex12*-null spermatocytes showed that they differed significantly (P<0.0001 and P=0.0002, respectively, Mann–Whitney test). Thus, TEX12 and SYCE2 are crucial for spatial confinement of the N-terminal region of SYCP1 and SYCE1 to a central position in between the axis of chromosomes.

DISCUSSION

The synaptonemal complex brings the homologous chromosomes in close apposition, regulating synapsis and maturation of cross-over recombination events. Genetic studies using knockout models, as well as immunoelectron microscopy localization studies, have identified four central element proteins (SYCE1, SYCE2, SYCE2 and TEX12) that contribute to synaptonemal complex formation and synapsis in mice (Fraune et al., 2012).

The role of central region proteins in stabilization of transverse filaments

Stabilization of transverse filaments across the central region of the synaptonemal complex is crucial in order to achieve synapsis between homologous chromosomes. Studies of the synaptonemal complex assembly process in *Syce3*-null and *Syce1*-null meiocytes have shown that interactions between opposing N-terminal regions of SYCP1 are not sufficient for synapsis initiation (Bolcun-Filas et al., 2009; Schramm et al., 2011). Instead, it has been proposed, based on the short central-element-like structures observed in between homologous chromosomes in *Syce2*-null and *Tex12*-null meiocytes, that SYCE3 and SYCE1 stabilize the N-terminal regions of SYCP1 within the central element, forming short synapsed regions along the paired homologous chromosomes (Costa and Cooke, 2007; Fraune et al., 2012). The recruitment of SYCE2 and TEX12 to the protein complex formed by SYCP1, SYCE3 and SYCE1 would then promote synaptonemal complex extension and synapsis. Importantly, we show here that SYCE1 and SYCE3 are not sufficient for stabilization of opposing N-terminal regions of SYCP1 at a central position between closely aligned axial structures. Instead, displacement of SYCE2 and TEX12 from the synaptonemal complex in *Tex12*-null spermatocytes results in a random distribution of the N-terminal region of SYCP1 and SYCE1 in between aligned lateral elements. Thus, we observed no evidence that a central element structure formed in *Tex12*-null meiocytes. Our results therefore suggest that SYCE2 and TEX12, together with SYCE3 and SYCE1, are necessary for transverse stabilization of N-terminal regions of SYCP1 within the central element and for synaptonemal complex extension between aligned homologous chromosomes (Fig. 5).

We have also analyzed the nature of the protein interactions that contribute to formation of the central element and the stabilization of the N-terminal regions of SYCP1 within the synaptonemal complex. A modular organization for central element assembly in mice has previously been indicated based on protein interaction experiments and knockout data, involving SYCE3–SYCE1 (Bolcun-Filas et al., 2009; Lu et al., 2014; Schramm et al., 2011) and SYCE2–TEX12 (Bolcun-Filas et al., 2007; Davies et al., 2012; Hamer et al., 2006, 2008). We show here that SYCP1 interacts with SYCE3 *in vitro* and when coexpressed in mammalian cell culture cells, that the localization of SYCE3 and the N-terminal region of SYCP1 overlap in a lateral view of the central element, and that SYCE3 recruits SYCE1 to filamentous structures formed by SYCP1 when coexpressed in mammalian cell culture cells. Thus,

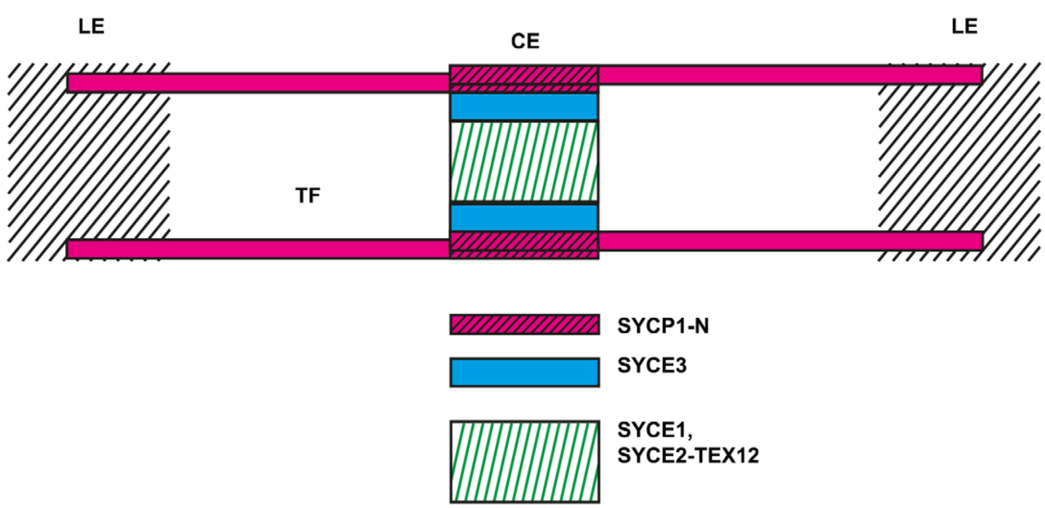

Fig. 5. A model for the organization of the central element of the synaptonemal complex in a lateral view. A cross section of the synaptonemal complex (including a lateral view of the synaptonemal complex) is displayed in order to view the organization of the proteins that constitute the central element (CE). We find that the N-terminal regions of the transverse filaments (TF; as defined by SYCP1) and SYCE3 are localized at the top and bottom edges of the central element, whereas SYCE1 and SYCE2 (and most likely also TEX12) are localized between the two layers defined by SYCP1-N and SYCE3. The N-terminal regions of opposing transverse filaments within the central element are presented in an overlapping manner, but head-to-head interaction cannot be excluded. The organization of the transverse filaments where they insert into the lateral element (LE; the C-terminal regions of SYCP1 molecules) is represented as an extrapolation of their organization at the central element and is based on earlier published data on well-defined multilayered synaptonemal complexes in other organisms (Schmekel et al., 1993a,b). The epitope regions within SYCE1, SYCE2 and SYCE3, and the N-terminal region of SYCP1, recognized by the primary antibodies used in this study are summarized in Fig. S2.

Journal of Cell Science (2016) 129, 2239-2249 doi:10.1242/jcs.182477

our results strongly suggest that SYCE3, through interactions with the N-terminal region of SYCP1 and with SYCE1, promotes assembly of a transverse-filament–central-element junction complex (Fig. 5).

Our results add to a growing knowledge of the molecular processes that guide synaptonemal complex assembly. It has been shown that the N-terminal region of C(3)G is crucial for transverse stabilization in *D. melanogaster* (Jeffress et al., 2007), and that transverse stabilization of C(3)G and synaptonemal complex extension require CONA and Corolla (Collins et al., 2014; Page et al., 2008). In *S. cerevisiae*, N-terminal deletions of ZIP1 only have minor effects on synaptonemal complex formation *in vivo* (Tung and Roeder, 1998), whereas Ecm11 and Gmc2 promote synaptonemal complex extension along the paired homologous chromosomes (Humphryes et al., 2013; Voelkel-Meiman et al., 2013). In *C. elegans*, four interdependent proteins (SYP1-1, SYP-2, SYP-3 and SYP-4) form a transverse filament-like structure that is essential for synaptonemal complex extension and synapsis (Colaiacovo et al., 2003; MacQueen et al., 2002; Schild-Prufert et al., 2011; Smolikov et al., 2007, 2009). An emerging picture is that categorizing synaptonemal complex proteins as either transverse filament or central element proteins seems somewhat arbitrary and possibly misguiding, as these proteins jointly contribute to transverse filament organization and stabilization, as well as central element formation and synaptonemal complex assembly, generating a conserved structure with similar dimensions in different organisms.

The central element of the synaptonemal complex in mice has a bilayered organization

Electron microscopy tomography studies have shown that the central element of the synaptonemal complex in insects has a multi-layered organization, comprising identical structural units stacked on top of each other (Schmekel and Daneholt, 1995). A structural unit comprises opposing transverse filaments linked together within the central element by symmetrically arranged pillars, and a fibrous network that connect the transverse filaments and the pillars within and between layers of structural units. Studies in *C. elegans* and *D. melanogaster* using immunoelectron microscopy and structured illumination microscopy have suggested that central region proteins could contribute to the formation of a layered organization (Collins et al., 2014; Lake and Hawley, 2012; Schild-Prufert et al., 2011).

It has not been possible using electron microscopy tomography to determine whether or not the central element in mammalian cells has a multi-layered organization (Schmekel et al., 1993a). We have here analyzed the molecular organization of the central element in mice with immunoelectron microscopy. Analysis of the distribution of gold particles representing the central element proteins and the N-terminal region of SYCP1 in a lateral view of the synaptonemal complex identified a bimodal pattern for SYCE3 and the N-terminal region of SYCP1, and a monomodal distribution pattern for SYCE1 and SYCE2. Our results therefore suggest that the central element of the synaptonemal complex in mice has a bilayered organization, with structural units formed by the N-terminal region of SYCP1 and SYCE3 stacked on top of each other, and with SYCE1, SYCE2 and TEX12 localized in between the two layers, establishing a junction complex (Fig. 5).

Analysis of the lateral organization of the synaptonemal complex in mice using dSTORM has identified a bimodal distribution pattern for the N-terminal region of SYCP1, SYCE1, SYCE2 and SYCE3 within the central element (Schucker et al., 2015). A colocalization of the known central element proteins within each of the two layers (Schucker et al., 2015), however, raises a question regarding the nature of the molecules that keeps the layers together in a lateral view. We show here by immunoelectron microscopy that SYCE1 and SYCE2 show a monomodal distribution pattern in between the layers defined by the N-terminal region of SYCP1 and SYCE3, suggesting that SYCE1 and SYCE2 support vertical stability between the two layers. How could the differences in results for the dSTORM experiments and our immunoelectron microscopy analysis of the central element of the synaptonemal complex be explained? We have in our study used seminiferous tubules that were chemically fixed following retrieval from the testis, Lowicryl-embedded and then serial sectioned, allowing us to follow the helical turns of the synaptonemal complex within individual pachytene cells in three dimensions. In the dSTORM analysis (Schucker et al., 2015), spermatocytes are physically expelled from the seminiferous tubules, spread, chemically fixed and then dried down on slides. Synaptonemal complex structures that showed local bubbles (assumed to represent synaptonemal complex twisted regions) were then analyzed to describe the lateral organization of the synaptonemal complex. It has previously been shown that ultrathin sections of Lowicryl-embedded seminiferous tubules provide a more reliable technical approach for high-resolution immunolocalization studies than the use of surface-spread spermatocytes (Schmekel et al., 1996). It cannot therefore be excluded in the high-resolution immunolocalization studies of the synaptonemal complex using dSTORM (Schucker et al., 2015) that the bimodal distribution of SYCE1, SYCE2, SYCE3 and the N-terminal region of SYCP1 observed within bubbles and that are associated with the synaptonemal complex results from a loss of synaptonemal complex integrity and/or epitope access.

The results of our immunoelectron microscopy analysis of the organization of the central element of the synaptonemal complex can only be indirectly compared with the three-dimensional structural model of the central region that has been proposed based on electron microscopy tomography experiments (Schmekel et al., 1993a). The bimodal distribution patterns for the N-terminal region of SYCP1 and SYCE3 and their ability to interact, however, suggest that these two proteins could contribute to formation of the pillars associated with the transverse filaments within the central element of the synaptonemal complex (Schmekel et al., 1993a). Furthermore, the interactions identified between SYCE3 and SYCE1 in multiple assays (Lu et al., 2014; Schramm et al., 2011) and the ability of SYCE3 to recruit SYCE1 to filamentous structures formed by SYCP1 as shown here, together with the monomodal distribution pattern for SYCE1 in between the layers defined by SYCE3, suggest that interactions between SYCE3 and SYCE1 provide vertical connections between layers. SYCE3 would then have a role similar to the one proposed for Corolla in connecting the N-terminal region of C(3)G and CONA (Collins et al., 2014). The monomodal distribution pattern observed for SYCE2 in between the two layers that are defined by the N-terminal region of SYCP1 and SYCE3 suggests that SYCE2 (and TEX12) contribute to formation of the filamentous structures observed in between the layers established by transverse filaments in electron microscopy tomography experiments (Schmekel et al., 1993a). The protein interactions that mediate the integration of SYCE2 and TEX12 in between the bilayered structure established by the N-terminal region of SYCP1 and SYCE3 remain to be identified. Further work using high-resolution cryoelectron-microscopy–tomography and crystallography will be required to define the molecular organization of the central element in more detail, combined with the use of Fab fragments derived from domain-

Journal of Cell Science (2016) 129, 2239-2249 doi:10.1242/jcs.182477

specific antibodies to improve lateral resolution in immunoelectron microscopy and super-resolution microscopy studies.

In conclusion, we show that TEX12 and SYCE2, in addition to SYCE3 and SYCE1, are required for stabilization of the N-terminal region of SYCP1 within the central element of the synaptonemal complex and for synaptonemal complex extension. We find that the central element of the synaptonemal complex in mice has a layered organization, where the N-terminal region of SYCP1 together with SYCE3 defines two layers stacked on top of each other. Importantly, SYCE1 and SYCE2 (and presumably also TEX12) localize between the two layers of transverse filaments, suggesting that they stabilize vertical contacts between the layers.

MATERIALS AND METHODS

Immunoelectron microscopy preparations

Samples were processed according to standard protocols as follows. Small fragments of mice testes were fixed with 4% paraformaldehyde for 2 h on ice, rinsed with cacodylate buffer, dehydrated through graded methanol solutions at 4°C, embedded in Lowicryl HM23 and polymerized in a UV chamber for 48 h at −20°C and then for 24 h at room temperature. Semi-thin sections (500 nm) of the resin-embedded testis were performed in order to identify seminiferous tubules at stages IV–VIII of the seminiferous epithelial cycle, stages at which primary spermatocytes are at the pachytene stage. Once identified, the seminiferous tubules with pachytene cells were pinpointed at the surface of the resin block and 80-nm ultrathin sections were cut for immunoelectron microscopy experiments. Resin blocks were cut with an ultra-microtome (Leica), and 80-nm ultrathin sections were collected on formvar–carbon-coated one-slot gold grids (Agar Scientific). Incubation with the primary antibody was performed overnight at 4°C. Samples were washed five times for 5 min each time with PBS and incubated with the appropriate 5 nm gold-conjugated secondary antibody for 90 min at room temperature. Samples were then washed five times for 5 min each time with PBS, air-dried and contrasted with 3% uranyl acetate followed by lead citrate for 10 and 3 min respectively, before examination in a transmission electron microscope (Philips, CM120) at 100 kV.

The following primary antibodies were used at the indicated dilutions: guinea pig anti-SYCE1 at 1:100 (Hamer et al., 2006) (recognizing amino acids 302–329 of mouse SYCE1), guinea pig anti-SYCE2 at 1:100 (Hamer et al., 2006) (recognizing amino acids 1–28 of mouse SYCE2), polyclonal rabbit anti-SYCE3 at 1:100 (recognizing the full-length protein) (kindly provided by Yoshinori Watanabe, Institute of Molecular and Cellular Biosciences, Tokyo, Japan) and rabbit anti-N-SYCP1 (recognizing amino acids 53–128 of the N-terminal region of rat SYCP1 corresponding to amino acids 55–124 of mouse SYCP1) at 1:10 (Liu et al., 1996). The following secondary antibodies were used at the indicated dilutions: goat anti-rabbit IgG conjugated to 5-nm gold at 1:100 (SPI supplies) and goat anti-guinea pig IgG conjugated to 5-nm gold at 1:50 (SPI supplies). The frequency distributions for the gold grain positions were analyzed using Prism 6 (Graphpad Software). For the wild-type synaptonemal complex, the frequency distributions for SYCE1, SYCE2, SYCE3 and the N-terminal region of SYCP1 in frontal and lateral views were fitted with Gaussian curves, using the least square method. We constrained the mean values in fitting Gaussian curves to less than 50 for the frontal view and more than 0 for the lateral view. For the *Tex12*-null data, two models were compared for the best fit – the Gaussian curve and the random distribution (a straight line with a slope equal to 0). For both SYCP1 and SYCE1, the random distribution fitted better to the experimental data according to the Akaike's Informative Criteria (the probability is >95%).

In vitro GST pulldown assay and coexpression analysis

GST-fused central element proteins were expressed in *Escherichia coli* BL21 (DE3) and purified on glutathione magnetic beads (Thermo Scientific). FLAG-tagged SYCP1 (amino acids residues 1–400) was prepared by performing *in vitro* transcription and translation (Promega), and the protein was mixed with beads bound to each GST-fusion protein in 50 mM Tris-HCl (pH 7.5), 150 mM NaCl, 0.2% Triton X-100 and 5 mM EDTA. For coexpression of SYCP1 and central element proteins, COS-7 cells grown on coverslips were transfected by Lipofectamine (Invitrogen) with plasmids expressing the proteins under the CMV promoter. Cells were fixed with 2% formaldehyde and permeabilized with 0.1% Triton X-100 for immunolabeling.

Animals

Wild-type C57BL/6 and mutant mice were used in accordance with regulations provided by the animal ethics committee at Karolinska Institutet.

Acknowledgements

We thank Oleg Shupliakov for help with sample preparation (Swedish Research Council grant 80521101). The service of the Electron Tomography Facility at Karolinska Institutet is also acknowledged.

Competing interests

The authors declare no competing or financial interests.

Author contributions

A.H.-H and C.H. conceived the study; A.H.-H., S.M., T.F., A.K. and S.S. designed the methodology; A.H.-H., T.F., A.K. and S.M. performed experiments; C.H., A.H.-H. and B.D. wrote the original draft, reviewed and edited the manuscript; C.H. acquired funding; C.H. supervised the project; A.H.-H. and C.H. administered the project.

Funding

This work was supported by grants from the Swedish Cancer Society (Cancerfonden); the Swedish Research Council (Vetenskapsrådet); Torsten Söderbergs stiftelse; Knut och Alice Wallenbergs stiftelse; and Karolinska Institutet. This work was also supported by Japan Society for the Promotion of Science KAKENHI [grant number 25891015 (to T.F.)]; and by a grant from the Ministry of Education - Singapore [grant number MOE2012-T3-1-001 (to S.S.)].

Supplementary information

Supplementary information available online at
http://jcs.biologists.org/lookup/suppl/doi:10.1242/jcs.182477/-/DC1

References

Anderson, L. K., Royer, S. M., Page, S. L., McKim, K. S., Lai, A., Lilly, M. A. and Hawley, R. S. (2005). Juxtaposition of C(2)M and the transverse filament protein C(3)G within the central region of Drosophila synaptonemal complex. *Proc. Natl. Acad. Sci. USA* **102**, 4482-4487.

Bolcun-Filas, E., Costa, Y., Speed, R., Taggart, M., Benavente, R., De Rooij, D. G. and Cooke, H. J. (2007). SYCE2 is required for synaptonemal complex assembly, double strand break repair, and homologous recombination. *J. Cell Biol.* **176**, 741-747.

Bolcun-Filas, E., Hall, E., Speed, R., Taggart, M., Grey, C., de Massy, B., Benavente, R. and Cooke, H. J. (2009). Mutation of the mouse Syce1 gene disrupts synapsis and suggests a link between synaptonemal complex structural components and DNA repair. *PLoS Genet.* **5**, e1000393.

Colaiacovo, M. P., MacQueen, A. J., Martinez-Perez, E., McDonald, K., Adamo, A., La Volpe, A. and Villeneuve, A. M. (2003). Synaptonemal complex assembly in C. elegans is dispensable for loading strand-exchange proteins but critical for proper completion of recombination. *Dev. Cell* **5**, 463-474.

Collins, K. A., Unruh, J. R., Slaughter, B. D., Yu, Z., Lake, C. M., Nielsen, R. J., Box, K. S., Miller, D. E., Blumenstiel, J. P., Perera, A. G. et al. (2014). Corolla is a novel protein that contributes to the architecture of the synaptonemal complex of Drosophila. *Genetics* **198**, 219-228.

Costa, Y. and Cooke, H. J. (2007). Dissecting the mammalian synaptonemal complex using targeted mutations. *Chromosome Res.* **15**, 579-589.

Costa, Y., Speed, R., Ollinger, R., Alsheimer, M., Semple, C. A., Gautier, P., Maratou, K., Novak, I., Hoog, C., Benavente, R. et al. (2005). Two novel proteins recruited by synaptonemal complex protein 1 (SYCP1) are at the centre of meiosis. *J. Cell Sci.* **118**, 2755-2762.

Davies, O. R., Maman, J. D. and Pellegrini, L. (2012). Structural analysis of the human SYCE2-TEX12 complex provides molecular insights into synaptonemal complex assembly. *Open Biol.* **2**, 120099.

de Vries, F. A. T., de Boer, E., van den Bosch, M., Baarends, W. M., Ooms, M., Yuan, L., Liu, J.-G., van Zeeland, A. A., Heyting, C. and Pastink, A. (2005). Mouse Sycp1 functions in synaptonemal complex assembly, meiotic recombination, and XY body formation. *Genes Dev.* **19**, 1376-1389.

Dong, H. and Roeder, G. S. (2000). Organization of the yeast Zip1 protein within the central region of the synaptonemal complex. *J. Cell Biol.* **148**, 417-426.

Fraune, J., Schramm, S., Alsheimer, M. and Benavente, R. (2012). The mammalian synaptonemal complex: protein components, assembly and role in meiotic recombination. *Exp. Cell Res.* **318**, 1340-1346.

Hamer, G., Gell, K., Kouznetsova, A., Novak, I., Benavente, R. and Hoog, C. (2006). Characterization of a novel meiosis-specific protein within the central element of the synaptonemal complex. *J. Cell Sci.* **119**, 4025-4032.

Hamer, G., Wang, H., Bolcun-Filas, E., Cooke, H. J., Benavente, R. and Hoog, C. (2008). Progression of meiotic recombination requires structural maturation of the central element of the synaptonemal complex. *J. Cell Sci.* **121**, 2445-2451.
Handel, M. A. and Schimenti, J. C. (2010). Genetics of mammalian meiosis: regulation, dynamics and impact on fertility. *Nat. Rev. Genet.* **11**, 124-136.
Harris, L. J., Skaletsky, E. and McPherson, A. (1998). Crystallographic structure of an intact IgG1 monoclonal antibody. *J. Mol. Biol.* **275**, 861-872.
Hawley, R. S. (2011). Solving a meiotic LEGO(R) puzzle: transverse filaments and the assembly of the synaptonemal complex in Caenorhabditis elegans. *Genetics* **189**, 405-409.
Humphryes, N., Leung, W.-K., Argunhan, B., Terentyev, Y., Dvorackova, M. and Tsubouchi, H. (2013). The Ecm11-Gmc2 complex promotes synaptonemal complex formation through assembly of transverse filaments in budding yeast. *PLoS Genet.* **9**, e1003194.
Jeffress, J. K., Page, S. L., Royer, S. K., Belden, E. D., Blumenstiel, J. P., Anderson, L. K. and Hawley, R. S. (2007). The formation of the central element of the synaptonemal complex may occur by multiple mechanisms: the roles of the N- and C-terminal domains of the Drosophila C(3)G protein in mediating synapsis and recombination. *Genetics* **177**, 2445-2456.
Krijnse Locker, J. and Schmid, S. L. (2013). Integrated electron microscopy: super-duper resolution. *PLoS Biol.* **11**, e1001639.
Lake, C. M. and Hawley, R. S. (2012). The molecular control of meiotic chromosomal behavior: events in early meiotic prophase in Drosophila oocytes. *Annu. Rev. Physiol.* **74**, 425-451.
Liu, J.-G., Yuan, L., Brundell, E., Björkroth, B., Daneholt, B. and Höög, C. (1996). Localization of the N-terminus of SCP1 to the central element of the synaptonemal complex and evidence for direct interactions between the N-termini of SCP1 molecules organized head-to-head. *Exp. Cell Res.* **226**, 11-19.
Lu, J., Gu, Y., Feng, J., Zhou, W., Yang, X. and Shen, Y. (2014). Structural insight into the central element assembly of the synaptonemal complex. *Sci. Rep.* **4**, 7059.
MacQueen, A. J., Colaiacovo, M. P., McDonald, K. and Villeneuve, A. M. (2002). Synapsis-dependent and -independent mechanisms stabilize homolog pairing during meiotic prophase in C. elegans. *Genes Dev.* **16**, 2428-2442.
McNicoll, F., Stevense, M. and Jessberger, R. (2013). Cohesin in gametogenesis. *Curr. Top. Dev. Biol.* **102**, 1-34.
Meuwissen, R. L., Offenberg, H. H., Dietrich, A. J., Riesewijk, A., van Iersel, M. and Heyting, C. (1992). A coiled-coil related protein specific for synapsed regions of meiotic prophase chromosomes. *EMBO J.* **11**, 5091-5100.
Moses, M. J. (1956). Chromosomal structures in crayfish spermatocytes. *J. Biophys. Biochem. Cytol.* **2**, 215-218.
Nagaoka, S. I., Hassold, T. J. and Hunt, P. A. (2012). Human aneuploidy: mechanisms and new insights into an age-old problem. *Nat. Rev. Genet.* **13**, 493-504.
Newman, G. R. and Hobot, J. A. (2001). *Resin Microscopy and On-Section Immunocytochemistry*. Berlin: Springer.
Ollinger, R., Alsheimer, M. and Benavente, R. (2005). Mammalian protein SCP1 forms synaptonemal complex-like structures in the absence of meiotic chromosomes. *Mol. Biol. Cell* **16**, 212-217.
Osman, K., Sanchez-Moran, E., Higgins, J. D., Jones, G. H. and Franklin, F. C. H. (2006). Chromosome synapsis in Arabidopsis: analysis of the transverse filament protein ZYP1 reveals novel functions for the synaptonemal complex. *Chromosoma* **115**, 212-219.
Page, S. L. and Hawley, R. S. (2001). c(3)G encodes a Drosophila synaptonemal complex protein. *Genes Dev.* **15**, 3130-3143.
Page, S. L., Khetani, R. S., Lake, C. M., Nielsen, R. J., Jeffress, J. K., Warren, W. D., Bickel, S. E. and Hawley, R. S. (2008). Corona is required for higher-order assembly of transverse filaments into full-length synaptonemal complex in Drosophila oocytes. *PLoS Genet.* **4**, e1000194.
Rasmussen, S. W. (1976). The meiotic prophase in Bombyx mori females analyzed by three dimensional reconstructions of synaptonemal complexes. *Chromosoma* **54**, 245-293.
Roux, K. H. (1999). Immunoglobulin structure and function as revealed by electron microscopy. *Int. Arch. Allergy Immunol.* **120**, 85-99.
Schild-Prufert, K., Saito, T. T., Smolikov, S., Gu, Y., Hincapie, M., Hill, D. E., Vidal, M., McDonald, K. and Colaiacovo, M. P. (2011). Organization of the synaptonemal complex during meiosis in Caenorhabditis elegans. *Genetics* **189**, 411-421.
Schmekel, K. and Daneholt, B. (1995). The central region of the synaptonemal complex revealed in three dimensions. *Trends Cell Biol.* **5**, 239-242.
Schmekel, K., Skoglund, U. and Daneholt, B. (1993a). The three-dimensional structure of the central region in a synaptonemal complex: a comparison between rat and two insect species, Drosophila melanogaster and Blaps cribrosa. *Chromosoma* **102**, 682-692.
Schmekel, K., Wahrman, J., Skoglund, U. and Daneholt, B. (1993b). The central region of the synaptonemal complex in Blaps cribrosa studied by electron microscope tomography. *Chromosoma* **102**, 669-681.
Schmekel, K., Meuwissen, R. L. J., Dietrich, A. J. J., Vink, A. C. G., van Marle, J., van Veen, H. and Heyting, C. (1996). Organization of SCP1 protein molecules within synaptonemal complexes of the rat. *Exp. Cell Res.* **226**, 20-30.
Schramm, S., Fraune, J., Naumann, R., Hernandez-Hernandez, A., Höög, C., Cooke, H. J., Alsheimer, M. and Benavente, R. (2011). A novel mouse synaptonemal complex protein is essential for loading of central element proteins, recombination, and fertility. *PLoS Genet.* **7**, e1002088.
Schucker, K., Holm, T., Franke, C., Sauer, M. and Benavente, R. (2015). Elucidation of synaptonemal complex organization by super-resolution imaging with isotropic resolution. *Proc. Natl. Acad. Sci. USA* **112**, 2029-2033.
Smolikov, S., Eizinger, A., Hurlburt, A., Rogers, E., Villeneuve, A. M. and Colaiacovo, M. P. (2007). Synapsis-defective mutants reveal a correlation between chromosome conformation and the mode of double-strand break repair during Caenorhabditis elegans meiosis. *Genetics* **176**, 2027-2033.
Smolikov, S., Schild-Prüfert, K. and Colaiacovo, M. P. (2009). A yeast two-hybrid screen for SYP-3 interactors identifies SYP-4, a component required for synaptonemal complex assembly and chiasma formation in Caenorhabditis elegans meiosis. *PLoS Genet.* **5**, e1000669.
Solari, A. J. and Moses, M. J. (1973). The structure of the central region in the synaptonemal complexes of hamster and cricket spermatocytes. *J. Cell Biol.* **56**, 145-152.
Sym, M., Engebrecht, J. A. and Roeder, G. S. (1993). ZIP1 is a synaptonemal complex protein required for meiotic chromosome synapsis. *Cell* **72**, 365-378.
Tung, K. S. and Roeder, G. S. (1998). Meiotic chromosome morphology and behavior in zip1 mutants of Saccharomyces cerevisiae. *Genetics* **149**, 817-832.
Voelkel-Meiman, K., Taylor, L. F., Mukherjee, P., Humphryes, N., Tsubouchi, H. and Macqueen, A. J. (2013). SUMO localizes to the central element of synaptonemal complex and is required for the full synapsis of meiotic chromosomes in budding yeast. *PLoS Genet.* **9**, e1003837.
Westergaard, M. and von Wettstein, D. (1972). The synaptinemal complex. *Annu. Rev. Genet.* **6**, 71-110.
Wolf, E., Kastner, B. and Luhrmann, R. (2012). Antisense-targeted immuno-EM localization of the pre-mRNA path in the spliceosomal C complex. *RNA* **18**, 1347-1357.
Yuan, L., Brundell, E. and Höög, C. (1996). Expression of the meiosis-specific synaptonemal complex protein 1 in a heterologous system results in the formation of large protein structures. *Exp. Cell Res.* **229**, 272-275.
Zickler, D. and Kleckner, N. (1999). Meiotic chromosomes: integrating structure and function. *Annu. Rev. Genet.* **33**, 603-754.
Zickler, D. and Kleckner, N. (2015). Recombination, pairing, and synapsis of homologs during meiosis. *Cold Spring Harb. Perspect. Biol.* **7**, a016626.